TECHNICAL BULLETIN NO. 62 DECEMBER 1965

The Genesis of Halloysite and Gibbsite from Mugearite on the Island of Maui

MARTHA T. NAKAMURA
and
G. DONALD SHERMAN

HAWAII AGRICULTURAL EXPERIMENT STATION, UNIVERSITY OF HAWAII

CONTENTS

Illustrations

(Continued)

CONTENTS, Continued

ACKNOWLEDGMENT

We wish to thank Dr. Goro Uehara of the Department of Agronomy and Soil Science who gave so much of his time in discussing many aspects of the problem, and Mr. Haruyoshi Ikawa, also of the Department of Agronomy and Soil Science, who prepared the electron micrographs and aided in interpreting them. The courtesy of the Electron Microscopy Section, Mineral Constitution Laboratories, College of Mineral Industries, Pennsylvania State University, in permitting the use of the micrographs is also appreciated.

THE AUTHORS

Martha T. Nakamura is Junior Soil Scientist at the Hawaii Agricultural Experiment Station.

Dr. G. Donald Sherman, Associate Director of the Hawaii Agricultural Experiment Station, is Senior Soil Scientist at the Hawaii Agricultural Experiment Station and Senior Professor of Soil Science, University of Hawaii.

The Genesis of Halloysite and Gibbsite from Mugearite on the Island of Maui

MARTHA T. NAKAMURA and G. DONALD SHERMAN

INTRODUCTION

There have been a number of studies on soil profile composition and genesis in the Hawaiian Islands, beginning with that of McGeorge (1917) and followed by those of Hough and Byers (1937), and Hough *et al.* (1941), Sherman and associates (1948, 1955), G. Fujimoto *et al.* (1948), Tamura *et al.* (1953, 1955), and many others. However, the number of studies covering the immediate weathering products of Hawaiian parent rocks has been small.

Dean (1947) observed that pahoehoe lava weathered into soil colloids which were dominantly kaolinitic. The kaolin content gradually decreased as the surface horizon was approached. In a Paaloa soil profile the saprolite 30 feet below the surface contained 65% kaolin, but at the surface the kaolin content was only 20%. Dean postulated that kaolin was removed by chemical decomposition or by deflocculation with subsequent downward movement within the profile. On the other hand, in soils developed from volcanic ash or porous aa lava, the kaolin content was generally higher at the surface than in the lower horizons.

The role of rainfall in soil genesis in the Hawaiian Islands was investigated by Tanada (1951). A definite correlation was established between kaolin content and rainfall, the kaolin decreasing with increasing rainfall. Although the parent materials and their geological ages were given, no relationships between the parent materials and their immediate weathering products were drawn.

Sherman and Uehara (1956) investigated the influence of a weathering environment created by the supply and release of bases through leaching on secondary mineral formation from olivine basalt. Kaolin was found on the upper surface of the exfoliated layer and montmorillonite clay was found in the lower layer where bases accumulated.

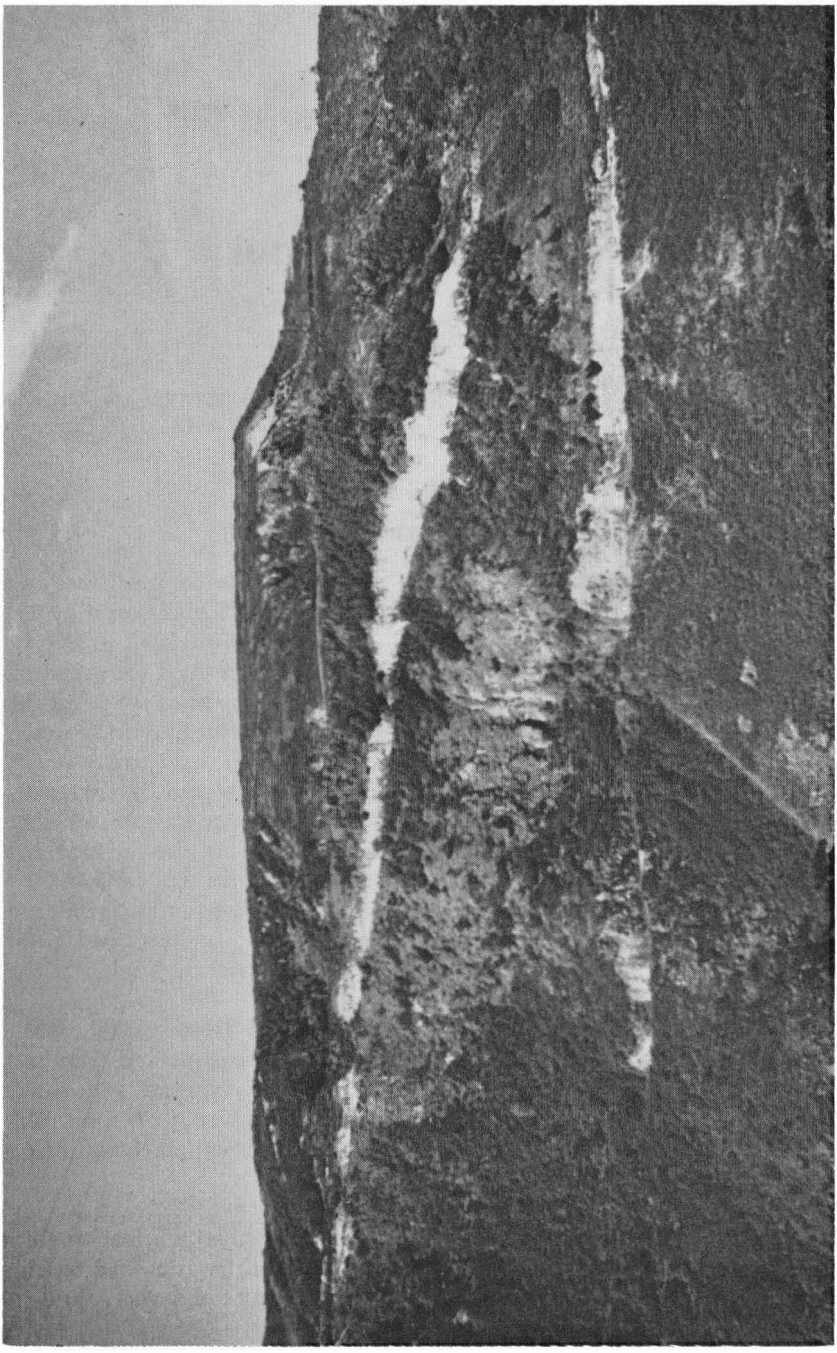

PLATE 1. Western wall of Wailena Gulch. The sample site is the white exposure midway along the inclined road leading to the Nobriga Ranch located at the top of the interfluve on the left of the photo.

Abbott (1958) studied gibbsite formation from olivine basalt on the island of Kauai and concluded that plagioclase feldspar weathered directly into gibbsite. He found that aluminum, in the final weathering stages, was mobilized and deposited along fractures and cavities to form gibbsite nodules.

Halloysite and gibbsite formation from mugearite on the island of Maui was studied by Bates (1962). He found that halloysite was formed from plagioclase feldspar subjected to desilication after the alkalies had been leached from it. The resultant halloysite was in turn weathered into gibbsite through further desilication.

Halloysite is an abundant 1:1 clay mineral found in Hawaiian soils, and this study covers its formation from mugearite in West Maui. The sample site is an easily accessible area of uncontaminated deep halloysite formation which can be readily seen by air travelers between Maui and Honolulu. In exposed roadcuts the geological formation gives the viewer an impression of extreme whiteness due to its contrast with the surroundings. Closer and more critical examination reveals variegated coloration, often indicative of the original structure. This site was selected for the sedentary character of its alteration from rock to soil.

Mugearite constitutes only a very minor portion of the parent rock in Hawaii. Extensive mugearite flows, however, have occurred in several places. The mugearite flow of the Honolua series, of which the sample area is a part, covers the original basalt over a large area in West Maui. Other areas in Hawaii where mugearite flows are found are in Molokai, where a relatively thin flow covers the basalt of East Molokai, and in Hawaii, where the mugearite flow of the Hawi volcanic series covers much of the western slope of Kohala Mountain (Macdonald, 1949).

Differential thermal, X-ray diffraction, chemical analyses, and light microscopy were utilized to characterize the weathering processes and products in the area. Electron microscopy was also used to a limited extent in this study.

DESCRIPTION OF THE SAMPLE SITE AND SAMPLES

The sample site is located on the north-northwestern end of West Maui, about eight miles from Waihee and is a road cut approximately 300 yards long. The road is cut into the steeply rising wall of the Wailena Gulch. The exposure is along an unpaved road leading to the Nobriga Ranch and runs in a south-southeasterly direction from an elevation above sea level of 700 feet to 775 feet. The actual sample site is midway along this roadway and is approximately 100 yards in length. A photograph of the sample site is reproduced in plate 1.

The soil in the site area belongs to the Halawa series of the Naiwa family and overlies the deep mugearite flow of the Honolua volcanic series. The exposure presents approximately 30 feet of this mugearite and its weathering products.

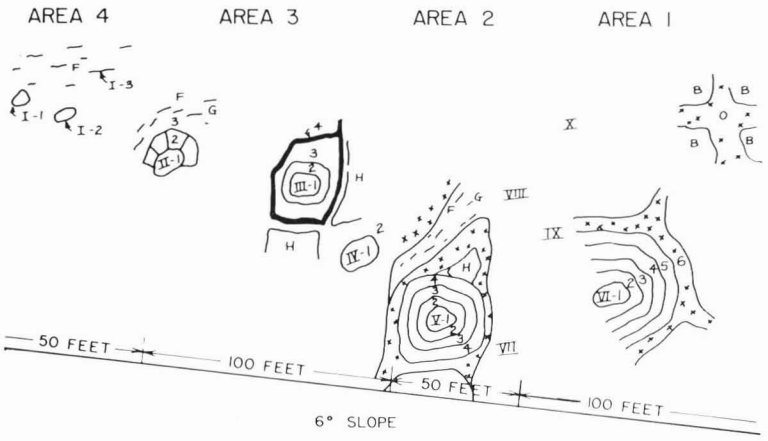

FIGURE 1. A diagrammatic sketch of the sample site and the samples collected within each area. F—friable material, G—gibbsite, H—halloysite, B—weathering boulder, X—vein halloysite.

The section of the exposure chosen as the sample site, which parallels the road at an inclination of approximately 6°, presents at its uppermost section a surface exposed to the weathering environment with development of pedological features. Gradually with descent the exposure becomes deeper and steeper, until it is predominantly rock weathering. However, since the exposure is along the walls of the interfluve, the weathering occurring at the sample site is actually one of surface function though it appears to be of depth function. The second ledge forms the surface of the uppermost section of the exposure giving rise to the Halawa soil series. Below this soil profile is an exposure of unweathered, as well as partially weathered, rocks and their products.

The study site was demarcated into areas representing these different weathering stages and representative samples were collected from each area. A diagrammatic sketch of the sample site is shown in figure 1.

Area 1 is a deep exposure at the lower end of the sample site and measures 100 feet along the road cut. This section shows the mugearite weathering to halloysite. Water percolating through the sample area moves more rapidly along any path which offers less resistance, such as the columnar and parallel platy joints found in mugearite. Weathering is then accelerated along these paths and as a result the mass is cut into blocks. When a small block is formed by such a process, the entire rock weathers homogeneously. When a larger section is cut off by the percolating water, the angles of the block are rounded and a spheroidal boulder is formed. The subsequent weathering within the boulder is not uniform. The outer portion separates into concentric shells since hydration and oxidation take place more rapidly on the outer surface of the block and create stress along this surface. This stress weakens the outermost portion of the boulder and creates additional paths for the

flow of water. This spalling process is repeated as further weathering goes on, resulting in boulders with several concentric shells, each shell at a different stage of weathering.

In addition to the downward flow of percolating water, there is also an outward concentration gradient of ions created in the boulder. This gradient causes dissolved ions to accumulate along the concentric radiating front. The accumulation from this outward diffusion is apparent in the dark-stained iron oxide rings which surround the exfoliating layers.

This weathering area has been designated area 1 in this study and sample VI, a vesicular rock and its exfoliating layers, labeled outward from the core as VI-2, -3, -4, and -5, as well as the halloysite of the drainage channel which set off this rock as a separate boulder, labeled VI-6, were obtained as a representative sample of this weathering stage. VI-1 $\wedge$ 2 and -4 $\wedge$ 5 interlayers are the dark iron-stained bands representative of the material which separates the exfoliating layers. Samples VIII, IX, and X were also taken from this area. The halloysite used as the standard in this study is from one of the large drainage channels of pure white halloysite from this sample area and is labeled "0" on the diagram.

In the section adjacent and above area 1, weathering has proceeded further and the bank is dominantly halloysite. The iron and titanium released in the weathering process have stained the bank brown and the color distinctly sets this area off from the adjacent area below it. There are unweathered to partially weathered rocks along the bank at the road level. This section is about 50 feet in length and has been designated area 2 in this study. Boulder V and its exfoliating layers are samples from area 2. The boulder was situated at the road level and below a large halloysite vein which was adjacent to a gibbsitic area. Sample series V consists of the unweathered core and three exfoliating layers collected from above and below the rock core. The samples are labeled upper and lower, respectively. A dark-colored layer sandwiched between exfoliating layers 2 and 3 was also collected.

Area 3, a dark brown-colored area of almost solid halloysite dissected by gibbsite, is about 100 feet long. The low-silica water percolating through the bank in some sections has through precipitation formed veins of light cream-colored gibbsite. Sample III is a halloysite disintegrating into friable material and set off by the gibbsite vein mentioned previously. Sample II was collected farther up within area 3. The core of halloysite was being desilicated along the conchoidal fractures, characteristic of halloysite, leaving a residue of yellow amorphous material. The material surrounding the halloysite core labeled II-3, is a dark brown-colored friable material interspersed with hardened stringers of yellow gibbsite.

At the end of the sample site and overlain by the Halawa soil profile is a bank of friable material about 50 feet in length, studded with gibbsite veinlets and nodules and halloysite fragments. The area is designated area 4 and samples I-1, I-2, I-3, representing agglutinated gibbsite, halloysite-like

material, and gibbsite stringers, respectively, are the representative fragments collected from this area.

EXPERIMENTAL DATA

Differential Thermal Analysis

Differential thermal analyses were made on all samples. To obtain quantitative measurements, the samples were first ground to pass a 100-mesh sieve. Four hundred milligrams of oven-dried sample was used in each case to eliminate weighing errors due to absorbed water. A heating rate of 15° C per minute was maintained throughout the analysis.

A quantitative estimation of halloysite was derived by comparing the area enclosed within the base line and the 590° C endotherm between the temperature limits of 450° to 650° C. A standard curve was obtained by running several differential thermal analyses on each of four samples weighing 100, 200, 300, and 400 milligrams, these weights representing 25%, 50%, 75%, and 100% halloysite, respectively. The area enclosed within the endothermic peak was measured with a planimeter and plotted as a function of mineral content. The resulting curve leveled off at the higher percentages but was linear between 25% and 75% clay content.

The standard sample used for the quantitative estimation of halloysite was the purest clay from the sample site. It is a dense, nonporous, porcelaneous, white clay from the drainage channels in area 1. The chemical analysis showed 40.35% SiO_2, 37.00% Al_2O_3, and 22.62% H_2O which resulted in a mole ratio of Al_2O_3:SiO_2:H_2O of 100:183:350. The silica-alumina ratio is lower than that of the porcelaneous samples of Ross and Kerr (1934) which was 191:100. Differential thermal curves of two standard halloysite minerals from Bedford, Indiana, and Eureka, Utah, were compared with this standard obtained from Maui. The comparative curves are given in figure 2. The available data indicate the Maui halloysite to be of high quality and hence represents a potential source of a good quantitative standard.

The standard for quantitative measure of gibbsite was a bauxite from Nadine, Georgia. Its endothermic peak was similar to the highest grade gibbsite obtained from the sample site of this study, sample III-4, a precipitated vein product from a drainage channel in area 3. The quantitative curve was derived by doing several differential thermal analyses on each of six samples containing 25, 50, 100, 150, 175, and 200 milligrams of standard gibbsite. The enclosed areas within the gibbsite endothermic peaks at 300° C were measured and plotted against the percentage of gibbsite to produce the standard curve. The resulting curve was also linear between 25% and 75% and leveled off at the higher concentrations.

The quantitative measurements of halloysite and gibbsite obtained by using these standard curves are tabulated in table 1. Also in the table is a tabulation of relative mineral content obtained by the X-ray diffraction data, which substantiates the differential thermal measurements. Where halloysite and gibbsite together do not add up to 100%, the difference may be

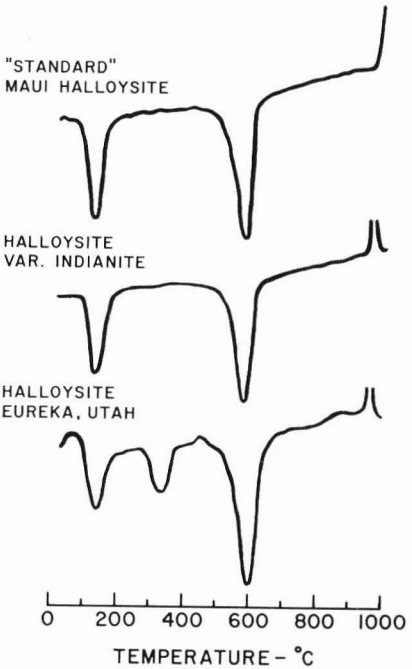

FIGURE 2. Differential thermograms comparing Maui halloysite with two standard halloysites.

attributed to the hydrated oxides of aluminum, iron, and titanium and amorphous hydrated silicates for which there is no quantitative method of measurement using the differential thermal apparatus.

Rock series VI from area 1 was found to have a slightly weathered core of amorphous material and halloysite. The halloysite content increased in the layer next to this core, VI-2. In the succeeding outer layers, VI-3, -4, -5, and -6, the samples contained from 80 to 85% halloysite. Differential thermal analyses indicated the presence of only halloysite and a small amount of amorphous material in this sample series.

Table 1 contains analyses of the exfoliating layers both above and below the unweathered core of sample series V from area 2. The upper layers were composed of gibbsite, amorphous material, and small amounts of halloysite. V-3 below the core was found to contain equal amounts of halloysite and gibbsite as well as amorphous material. The outermost or the fourth layer both above and below the core was predominantly halloysitic. The differential thermal curves of rock series V and VI are reproduced in figures 3 and 4, respectively.

Rock series II, III, and IV from area 3 represent cores of halloysite undergoing desilication to amorphous material and gibbsite. Samples I-1 and I-2 from area 4 both showed dominant gibbsite peaks with some halloysite.

TABLE 1. Halloysite and gibbsite content of the samples

SAMPLE NO.	DESCRIPTIVE NUMBER	DIFFERENTIAL THERMAL DATA		X-RAY DIFFRACTION DATA*		
		Halloysite (%)	Gibbsite (%)	Halloysite	Gibbsite	Feldspa
0	"standard" halloysite	100	0	XXXX		
1	I-1 cherty aggregate	26	78	X	XXXX	
2	I-2 porcelaneous material	18	64		XXXX	
3	I-3 stringer	—	—		XXXX	
4	II-1 light gray core	40	20	XX	XX	
5	II-2 "waxy" dark gray	70	0	XXX		
6	II-3 <2 mm fraction	tr	40		XX	
7	II-3 >2 mm fraction	tr	87		XXXX	
8	III-1 blue core	70	tr	XXXX		
9	III-2 "waxy" brown	60	tr	XXXX		
10	III-3 friable material	0	67		XXX	
11	III-4 cream-colored vein	tr	100		XXXX	
12	IV-1 white core	80	0	XXXX		
13	IV-2 friable material	15	52		XXX	
14	V-1U dense parent rock	0	0			XXXX
15	V-2U light gray-white	tr	20	X	X	XX
16a	V-2∧3a soft interlayer	tr	34	X	X	
16b	V-2∧3b dense interlayer	tr	0	X	X	
17	V-3U light gray	22	55	X	XXX	
18	V-4U "waxy" brown	82	0	XXXX		
19	V-2L	30	tr	XX	X	XX
20	V-3L	34	34	XX	XX	
21	V-4L	79	tr	XXXX	X	
22	VI-1 vesicular core	tr	0	X		XXX
23	VI-1∧2 interlayer	tr	0	X		XX
24	VI-2	33	0	XX		XX
25	VI-3	84	0	XXXX		
26	VI-4	85	0	XXXX		
27	VI-4∧5 interlayer	57	0	———		
28	VI-5	80	0	XXXX		
29	VI-6 vein material	85	0	XXXX		

* XXXX = dominant.
XXX = abundant.
XX = moderate.
X = detected.

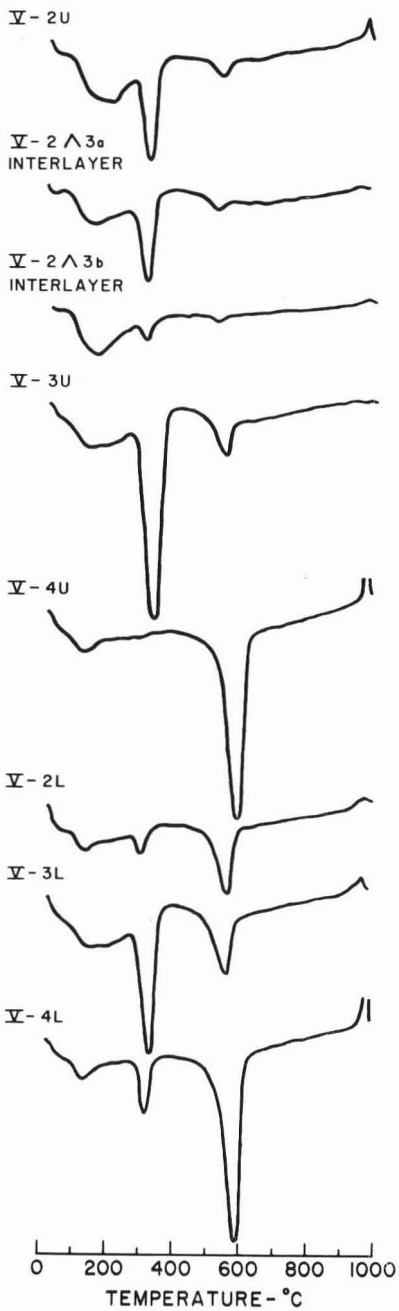

FIGURE 3. Differential thermal curves of sample series V.

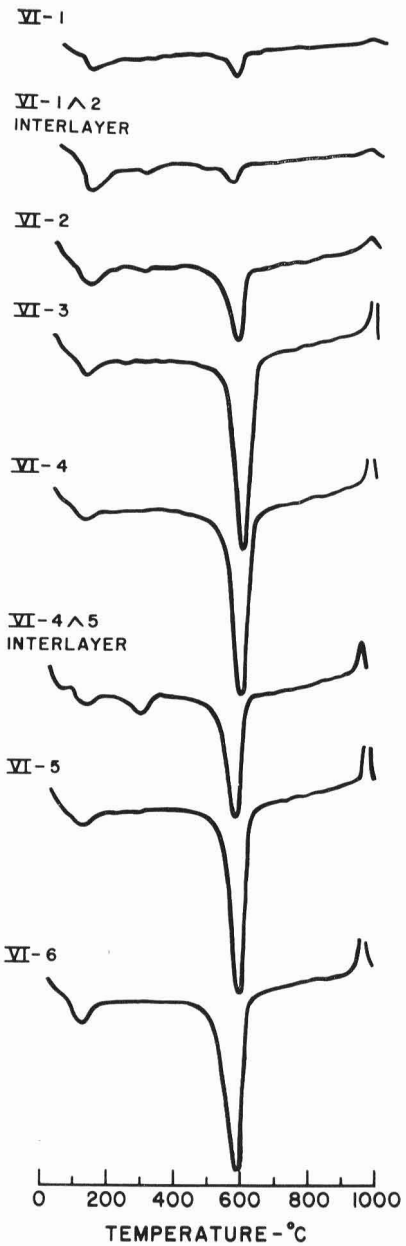

FIGURE 4. Differential thermal curves of sample series VI.

X-ray Diffraction Analysis

X-ray diffraction data for the samples were obtained on the Norelco diffractometer using copper K_α radiation and a nickel filter.

The X-ray diffraction patterns of the Maui halloysite "standard" are reproduced in figure 5. The powder sample formed peaks at 9.93Å, 4.39Å, and 3.36Å with a broad basal spacing. With ethylene glycol treatment, its (001) reflection shifted to 10.8Å. When heated, its (001) reflection moved to 7.25Å and formed a sharp peak. The foregoing patterns were repeated by all of the halloysite samples of this study, indicating that they were hydrated halloysite containing smaller amounts of the less hydrated form of the mineral.

The diffraction data on sample series VI showed a core of plagioclase feldspar and succeeding layers containing hydrated halloysite. These data were compiled from powdered, ethylene glycol solvated, and heated samples. Sample series V produced diffraction data indicating a predominance of gibbsite with some hydrated halloysite in all layers except the fourth layer which contained only halloysite. The diffraction data of sample series III shows halloysite weathering to gibbsite. The diffraction patterns for sample series V and VI are shown in figures 6 and 7, respectively.

Since the weathering pattern of boulder V differed from that of boulder VI, samples from the first weathering layers of several rocks from areas 1 and 2 were examined by X-ray diffraction. These data and microscope studies indicate that the feldspars in rock VII have weathered to halloysite, following a pattern similar to that in boulder VI. In the first dark layer of rock VIII, there was gibbsite in addition to the feldspar. The second layer of this rock was set off into a light-colored, low volume-weight section and a higher volume-weight section. Halloysite and some gibbsite were found in the low volume-weight section, whereas there was only halloysite in the other section. Rock IX was likewise divided into two weathering layers. The first or inner layer was composed of feldspar and a small amount of gibbsite. In the outer layer there was a larger amount of gibbsite and some feldspar. A faint clay line was also observed in the diffraction chart of this sample, although no definite peak at 7.25Å was observed. Rocks VIII and IX were thus similar to boulder V at its initial weathering stage, gibbsite being identifiable before a definite halloysite pattern is established. Rock X was the only vesicular rock examined. Feldspar and a clay line appeared in its diffraction chart. The foregoing samples showed different weathering patterns at the initial stage, but the fully weathered outer layers of the rocks were halloysite.

Chemical Analysis

Data obtained through chemical analysis are contained in table 2. When transferred to ternary diagrams, the results indicate a trend toward desilication.

In sample series VI (figure 8), the core has 62 mole percent SiO_2. The succeeding layers lost silica and molecular percentages of 16% Al_2O_3, 31%

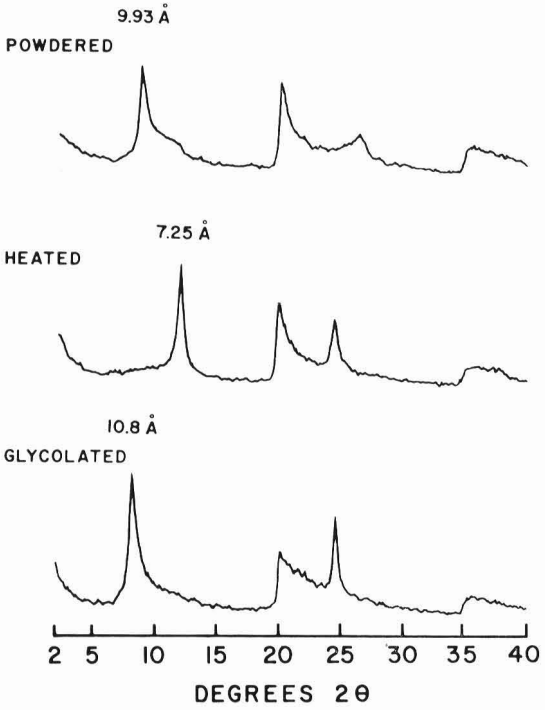

FIGURE 5. X-ray diffraction patterns of the Maui "standard" halloysite.

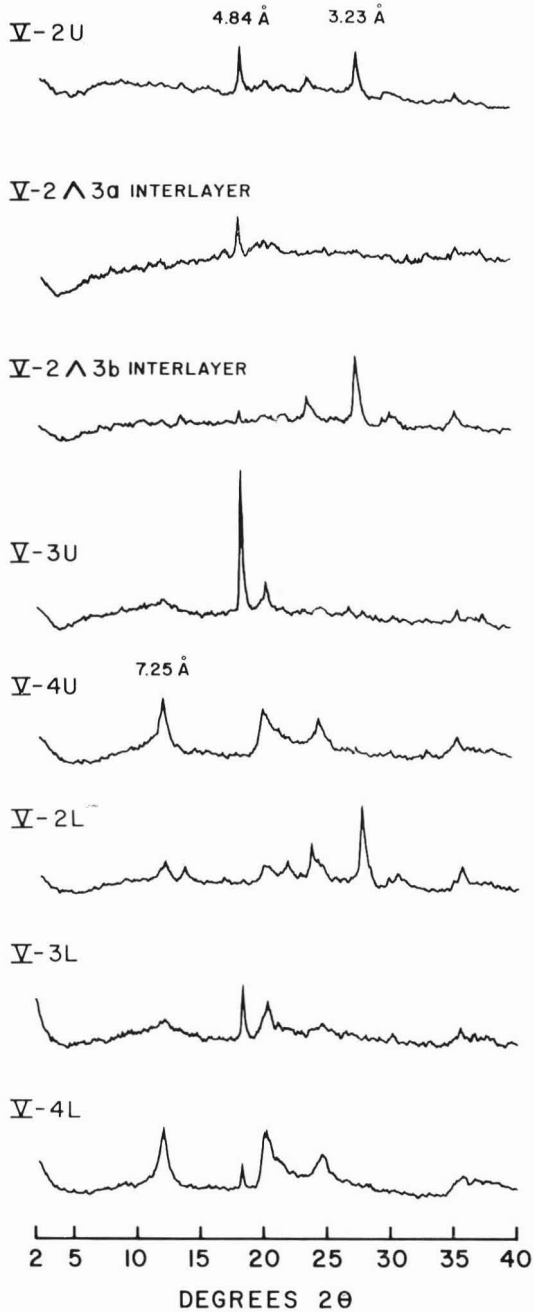

FIGURE 6. X-ray diffraction patterns of sample series V.

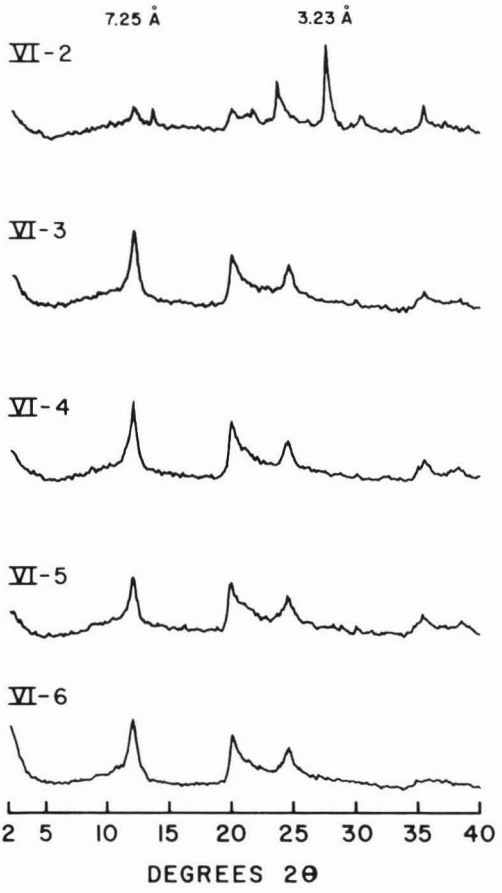

FIGURE 7. X-ray diffraction patterns of sample series VI.

TABLE 2. Chemical composition of the samples

SAMPLE NO.	DESCRIPTIVE NUMBER	SiO_2 (%)	TiO_2 (%)	Al_2O_3 (%)	Fe_2O_3 (%)	FeO (%)	MnO (%)	MgO (%)	CaO (%)	Na_2O (%)	K_2O (%)	P_2O_5 (%)	L.O.I. (%)	$H_2O(-)$ (%)	TOTAL
0	"Standard"	40.35	none	37.00	0.02	—	none	0.06	none	none	none	0.09	14.12	8.50	100.14
1	I-1	13.65	0.11	57.02	0.11	—	none	0.03	none	none	none	0.08	27.92	1.59	100.49
2	I-2	9.49	none	59.89	0.30	—	none	0.06	none	none	none	0.13	29.77	1.16	100.80
3	I-3*														
4	II-1	25.61	2.29	32.24	13.44	—	0.18	0.78	none	0.15	0.09	1.17	16.00	7.72	99.67
5	II-2	37.48	1.03	33.49	6.60	—	0.06	0.03	none	0.17	0.10	0.41	13.91	6.29	99.57
6	II-3<2 mm	9.42	3.66	32.29	20.93	—	0.50	1.38	none	0.14	0.09	1.93	20.28	9.47	100.09
7	II-3>2 mm	2.60	0.89	55.67	5.76	—	0.13	0.89	none	none	none	0.89	31.51	2.53	100.87
8	III-1	36.20	0.90	34.97	5.98	—	0.10	tr	none	0.10	none	0.40	14.38	6.72	99.75
9	III-2	34.02	1.04	33.88	7.07	—	0.10	0.02	none	0.02	none	0.70	14.63	8.18	99.66
10	III-3	4.40	2.63	46.17	12.54	—	0.37	0.86	none	0.03	0.02	1.45	25.66	5.94	100.07
11	III-4	3.88	0.43	59.40	1.13	—	0.03	0.05	none	0.09	0.02	0.48	31.95	2.81	100.27
12	IV-1	43.41	0.07	39.45	0.24	—	none	0.09	none	0.06	none	0.09	15.16	1.46	100.03
13	IV-2	8.20	1.70	48.76	9.70	—	0.24	0.57	none	0.04	none	0.24	26.49	4.32	100.26
14	V-1U	57.66	1.21	16.78	4.81	3.26	0.25	1.67	3.14	6.80	2.45	0.75	0.86	0.54	100.18
15	V-2U	28.94	2.47	30.00	7.60	0.75	0.12	0.63	0.24	1.41	1.10	1.55	16.56	9.28	100.65
16a	V-2∧3a	19.98	3.11	25.16	21.53	0.71	0.16	0.69	none	0.27	0.14	1.78	17.99	8.43	99.95
16b	V-2∧3b	42.05	1.59	22.04	10.61	0.45	0.09	0.68	0.76	3.34	1.99	1.00	9.41	6.08	100.26
17	V-3U	15.13	3.03	39.86	12.17	1.01	0.19	0.55	none	0.03	0.05	1.42	22.80	5.20	100.20
18	V-4U	36.80	1.11	33.21	8.33	0.26	0.10	0.21	none	0.27	none	0.70	13.98	5.65	100.62
19	V-2L	45.42	1.51	26.62	5.62	0.28	0.09	0.12	0.70	3.33	1.70	0.90	9.95	3.72	99.96
20	V-3L	21.60	2.34	37.76	5.41	0.47	0.11	0.35	none	0.24	0.18	1.69	19.50	10.67	100.32
21	V-4L	36.34	0.54	37.24	3.39	none	0.03	0.08	none	0.08	none	0.24	16.52	5.82	100.28
22	VI-1	54.27	1.55	22.73	4.08	none	0.33	0.34	1.00	5.98	2.67	0.67	3.93	2.15	99.70
23	VI-1∧2	44.37	4.53	18.84	13.07	none	0.31	0.55	0.38	4.18	2.16	1.32	6.07	4.23	100.01
24	VI-2	40.76	2.49	23.46	10.41	none	1.58	0.06	1.05	3.74	1.85	0.92	8.76	4.90	99.98
25	VI-3	38.46	1.29	33.61	5.63	none	0.24	0.10	none	0.06	none	0.18	13.74	6.81	100.12
26	VI-4	37.13	1.72	33.81	6.76	none	0.10	tr	none	0.11	none	0.20	13.59	6.28	99.50
27	VI-4∧5	27.68	1.93	22.50	27.81	none	0.18	0.05	none	0.14	none	0.92	12.93	6.04	100.18
28	VI-5	37.01	2.03	32.62	9.14	none	0.07	tr	none	0.15	0.07	0.29	13.38	5.63	100.39
29	VI-6	38.68	0.63	34.98	0.92	none	0.05	tr	none	0.97	none	0.13	15.79	8.42	100.57

* Sample not analyzed.

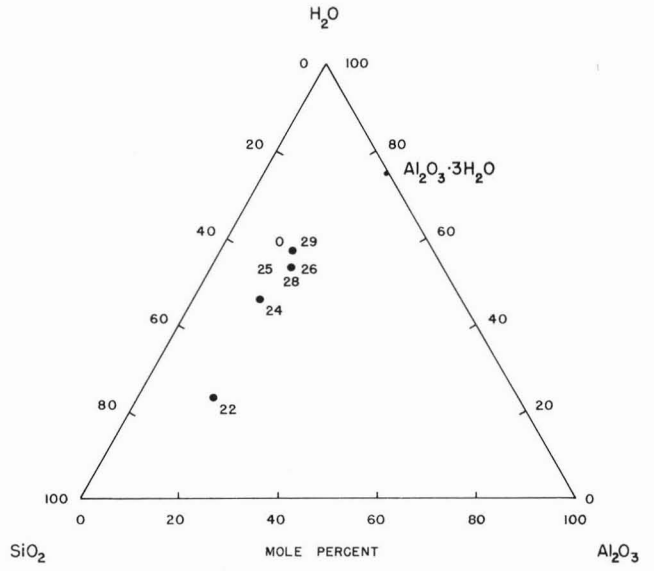

FIGURE 8. Ternary diagram of sample series VI, showing desilication and formation of halloysite. The number "0" is sample 0, the "standard" halloysite.

SiO_2, and 52% H_2O were reached in the third, fourth, and fifth exfoliating layers. These samples are residual halloysites. VI-6, taken from a vein, has molecular percentages of 15% Al_2O_3, 28% SiO_2, and 57% H_2O, identical with the percentages of the "standard," a vein halloysite also. The molecular percentages of these two samples are very close to the theoretical percentages for halloysite, i.e., 14% Al_2O_3, 29% SiO_2, and 57% H_2O. The graph indicates the process to be one of loss of silica and of gain in water, with very little change in the alumina content.

Figure 9 is the ternary diagram for sample series V. The plots for the overlying exfoliating layers of sample series V are represented by dots while those for the lower layers are designated as circles. The diagram confirms that these layers are following the same pattern of desilication, but that the upper layers are weathering at a slightly faster rate than their corresponding lower layers. Exceptions to the foregoing pattern are the fourth exfoliating layers (18 and 21) which are halloysites rather than gibbsite. The molecular percentages for sample 18 are 16% Al_2O_3, 31% SiO_2, and 53% H_2O, identical with the molecular percentages of the residual halloysites of series VI described in the preceding paragraph. Petrographic data corroborate the foregoing. The silica content in sample 21 is slightly lower than those in residual halloysites. The presence of gibbsite in a predominantly halloysite layer was confirmed by the petrographic data.

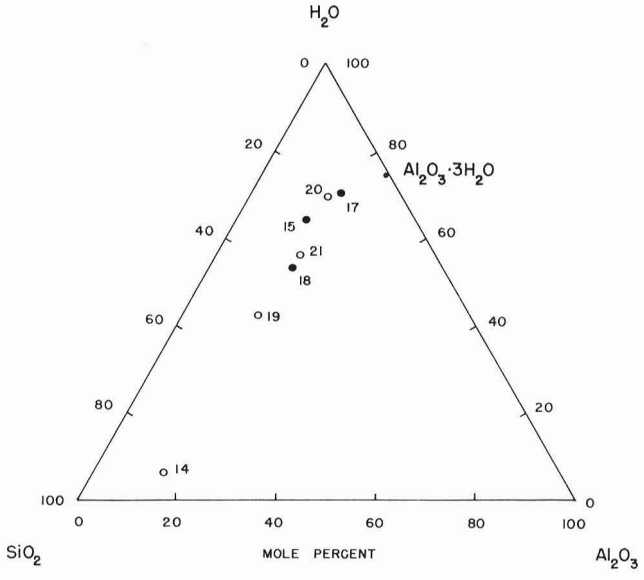

FIGURE 9. Ternary diagram of sample series V, showing halloysite formation by desilication. Dots represent the overlying exfoliating layers and circles represent the lower exfoliating layers. 14 is the unweathered rock.

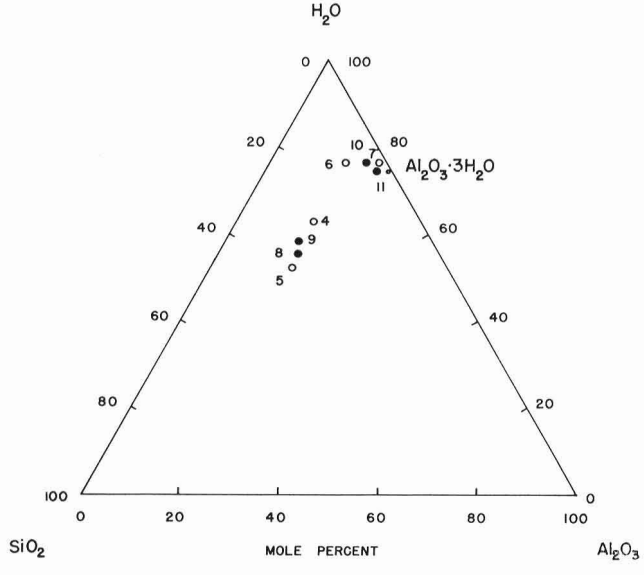

FIGURE 10. Ternary diagram of sample series II, represented by circles, and sample series III, represented by dots. The diagram shows both sample series undergoing gibbsitization.

The ternary diagram of sample series II and III (figure 10), both examples of desilication to gibbsite, indicates the initial stage of desilication to be that of a constant loss of silica with concomitant gain of water and the maintenance of alumina at approximately 15% until the maximum theoretical water percentage is reached. After this theoretical maximum is reached, the loss of silica continues, thereby concentrating alumina until the theoretical molecular percentage of gibbsite is approached. Silica, however, is never completely lost.

Petrographic Microscopy

Detailed petrographic studies of boulders V and VI were made to obtain their weathering sequences. Rock V was a dense mugearite and rock VI a vesicular mugearite. According to Stearns and Macdonald (1942), a mugearite has a matrix composed of sodic oligoclase feldspar arranged in a trachytic texture. The feldspar phenocrysts are calcic to intermediate oligoclase surrounded by thin shells of sodic oligoclase. Numerous acicular apatite crystals are enclosed in the feldspar. The mafic minerals which constitute 15–20% of the rock are olivine, pyroxene, and magnetite, as well as a little hornblende and biotite.

Boulder VI had a slightly weathered core. Most of the matrix plagioclase was still birefringent. The centers of the plagioclase phenocrysts were entirely isotropic, but often patches of isotropic and birefringent sections were observed (plate 2). The ferromagnesium minerals appeared unweathered. The vesicles were partially filled with a low color birefringent material oriented normal to the cavity walls and crescent-shaped iron oxide.

The original structure of sample VI-2 was almost obliterated and the groundmass was completely isotropic. The outlines of the plagioclase phenocrysts were no longer discernible; however, small amounts of unweathered fragments of feldspars could still be identified. The magnetites were prominent and most of the ferromagnesium minerals appeared unweathered. The secondary minerals in the vesicles were enlarged.

The third, fourth, and fifth exfoliating layers were completely isotropic showing the characteristic gray undulating extinction of halloysite. However, there were numerous low white birefringent streaks forming a reticular pattern, as shown in plate 2. The cavity fillings were well aggregated and appeared to be gibbsite. The ferromagnesium minerals seemed to have undergone some weathering. Most of the cleaved pieces of pyroxene still retained their high birefringence, whereas some of the fragments were mixtures of minute low birefringent and isotropic material. VI-6 was taken from the layer surrounding the boulder. This slide did not follow the preceding general pattern. It was completely isotropic with faint gray undulating extinction. No rock structure was visible. This was not residual material but precipitated halloysite.

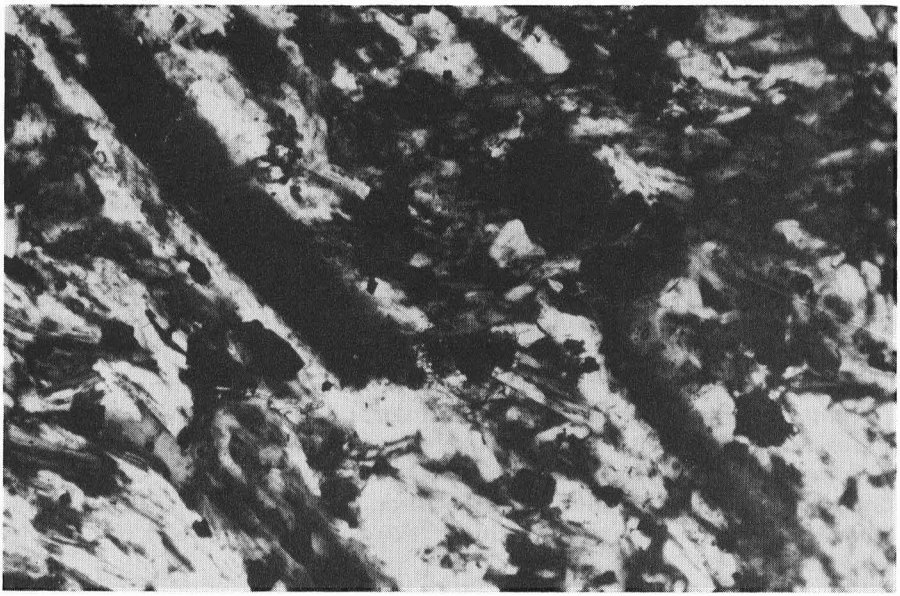

A. VI-1 Crossed-nicols × 140

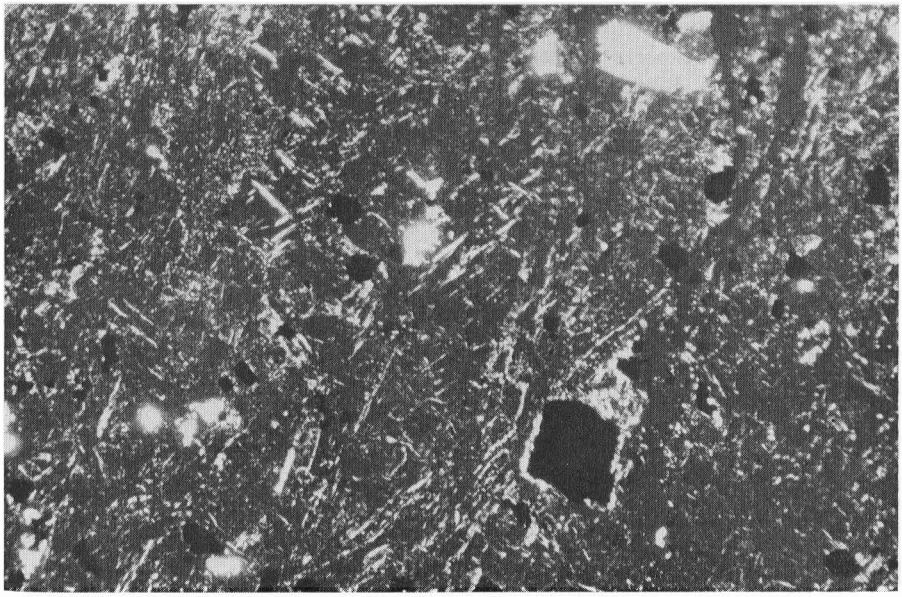

B. VI-4 Crossed-nicols × 140

PLATE 2. A—Isotropic plagioclase phenocryst and partially altered groundmass.
B—Completely isotropic halloysite with birefringent reticular pattern.

The rock of sample series V was dense mugearite, similar in composition to Macdonald's (1949) description of mugearite. The core was essentially unweathered. There was some chlorite scattered throughout the slide and the calcic center of a few of the huge phenocrysts had been altered into zeolite and calcite.

In the second exfoliating layer, most of the groundmass consisted of birefringent plagioclase and isotropic material. The plagioclase phenocrysts were isotropic, only the sodic oligoclase rim being unweathered. All of the ferromagnesium minerals were under various stages of weathering. They appeared as highly birefringent fragments or aggregates of very low birefringent micro-crystals showing a "salt-and-pepper" effect. Similar microcrystalline materials were also observed in some interstices of the plagioclase (plate 3).

Plate 4 is a section characteristic of the sample series V where gibbsitization retained the trachytic texture of the rock. The plagioclase phenocrysts were isotropic with gibbsite concentrated along the edges and the cleavage faces. Plate 5 shows the complete gibbsitization of the rock with secondary iron oxide also following the trachytic texture of the rock and paralleling the gibbsite.

The fourth exfoliating layers were quite unlike the others. Plate 6 is a photomicrograph of the lower section showing the isotropic halloysite with some gibbsite. The ferromagnesium phenocrysts are either all iron oxide or a mixture of heavily iron-stained gibbsite. The thin section of the upper layer showed a completely isotropic background with extinction characteristics of halloysite. Birefringent material in a fine reticular pattern appeared in this isotropic background. The placement of the visible minerals, including magnetite and ferromagnesium phenocrysts, seems to indicate that this was residual material. Petrographically, it looked much like rock series VI. This layer was located next to a leaching channel of high silica content and was therefore in an environment conducive to halloysite formation. This may have resulted in its being weathered into halloysite without following the gibbsitization process found in V-2 and V-3.

I-2 resembled a porcelaneous halloysite but was shown by all analyses to be gibbsite. The slide section (plate 7) shows the gibbsite appearing from the isotropic background as a result of desilication. Typical translocation forms of gibbsite crystals appear in the slide section of sample I-3, a stringer form of gibbsite. Faint gibbsite aggregation appears from the isotropic groundmass indicating its initial amorphous state and its subsequent crystallization to gibbsite.

Electron Microscopy

A few selected samples were examined with an electron microscope by Mr. Haruyoshi Ikawa of the Department of Agronomy and Soil Science during his study leave at Pennsylvania State University. The micrographs

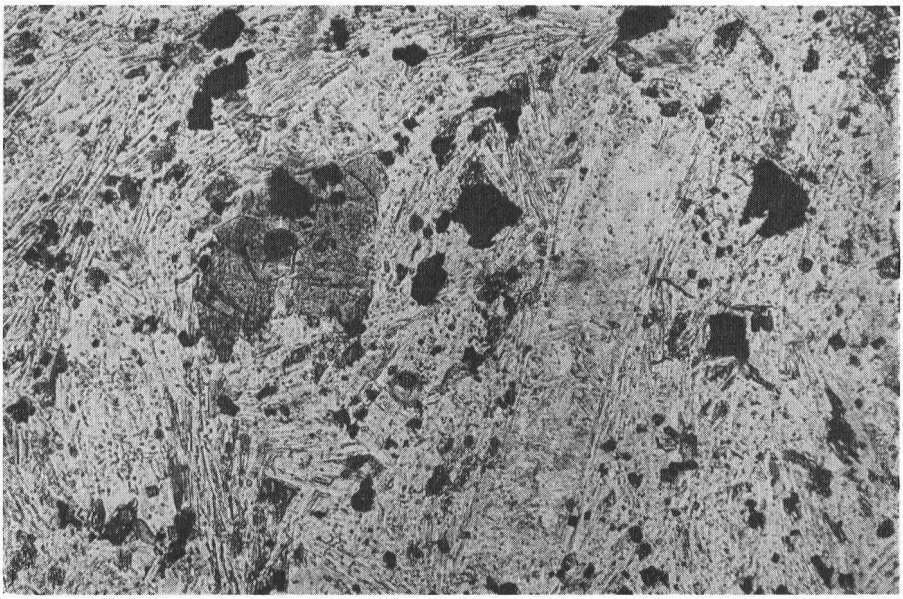

A. V-2 Lower Plain light × 140

B. V-2 Lower Crossed-nicols × 140

PLATE 3. Plagioclase phenocryst isotropic in the center with unweathered sodic rim. Groundmass plagioclase partially isotropic. Ferromagnesium minerals partially isotropic and showing salt-and-pepper effect.

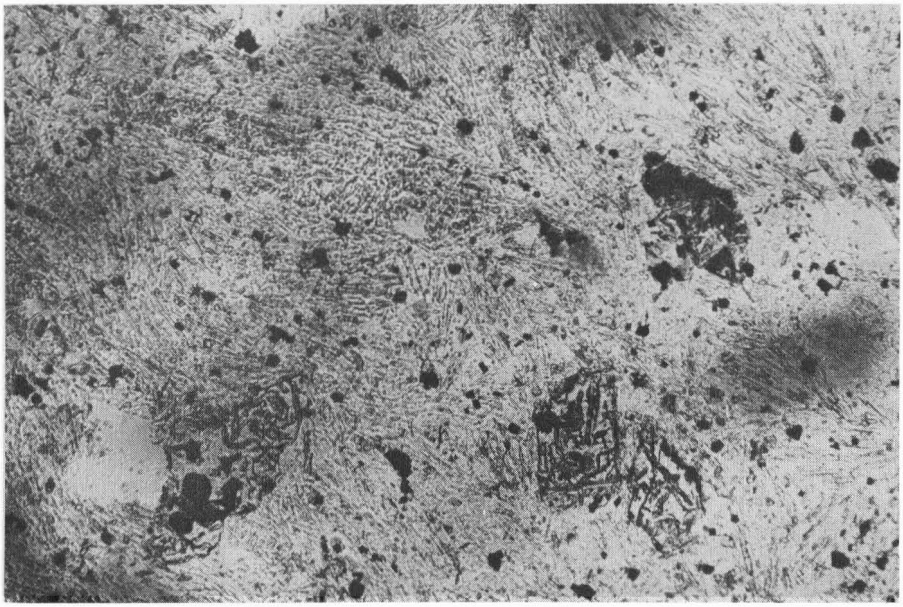

A. V-3 Lower Plain light × 140

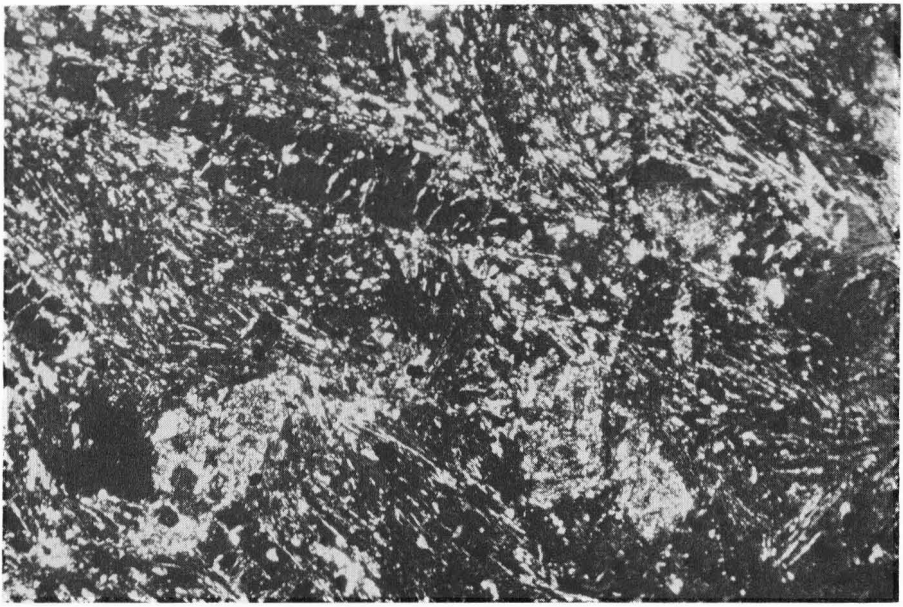

B. V-3 Lower Crossed-nicols × 140

PLATE 4. Dominantly isotropic plagioclase phenocryst. Gibbsitization of the ferromagnesium minerals and the groundmass feldspar.

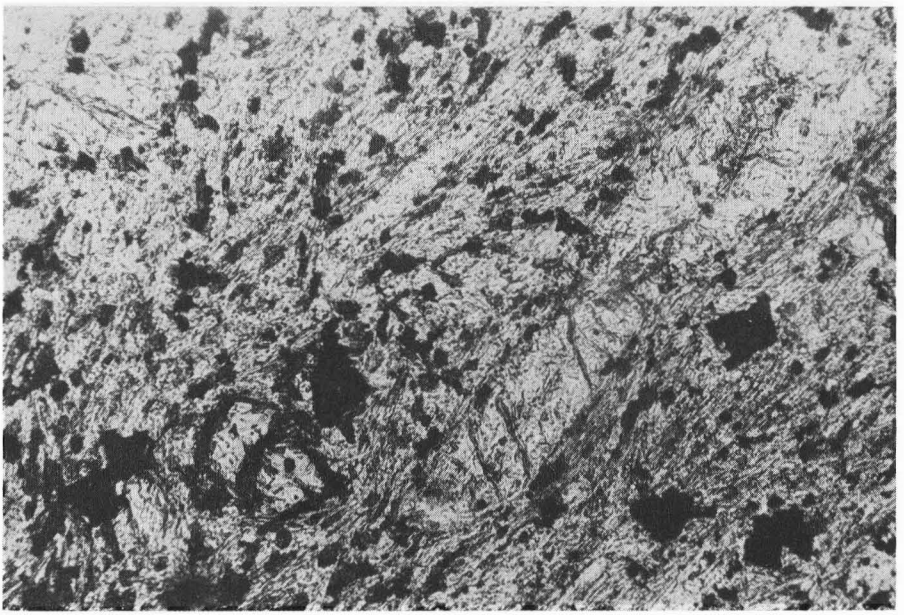

A. V-3 Upper Plain light × 140

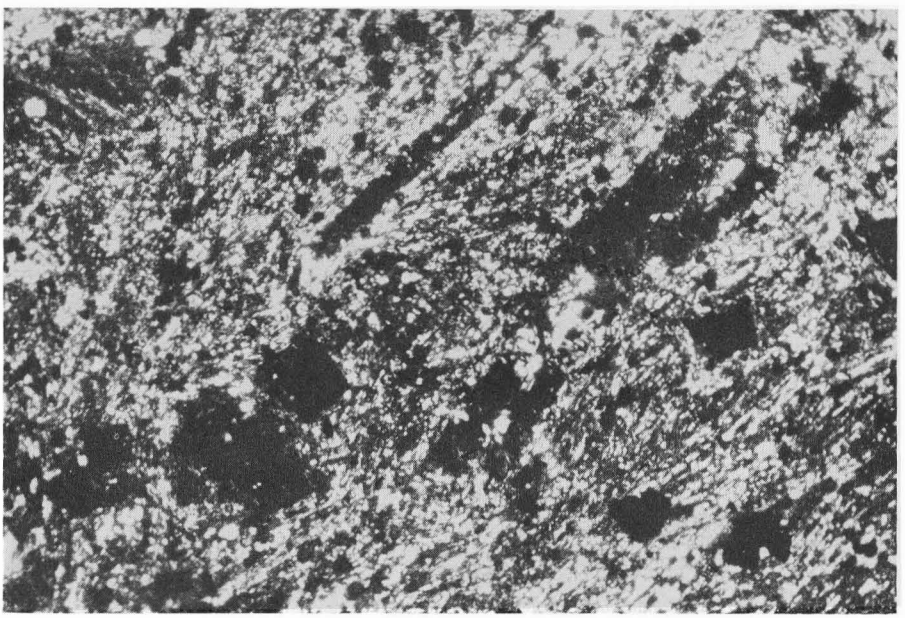

B. V-3 Upper Crossed-nicols × 140

PLATE 5. Completely gibbsitized rock, retaining the original trachytic texture.

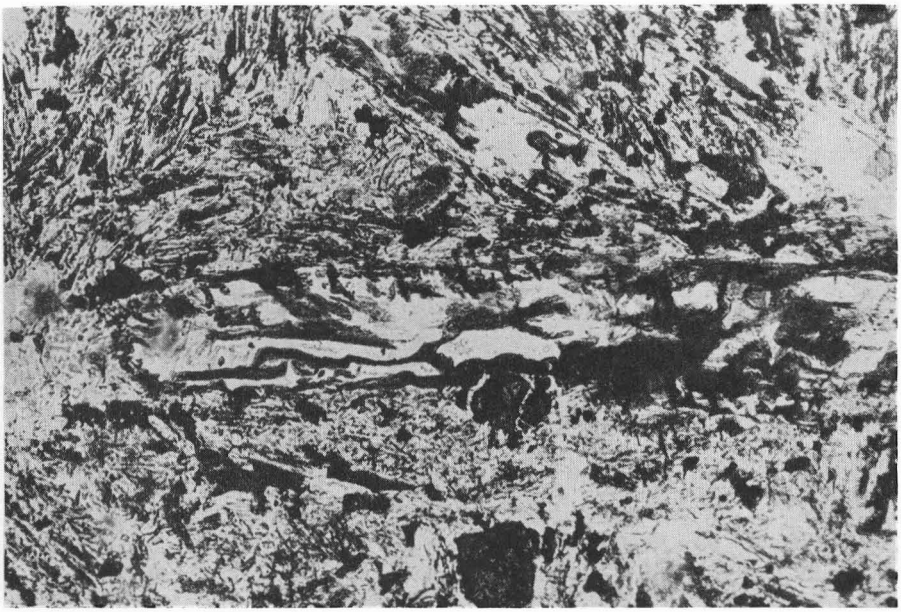

A. V-4 Lower Plain light × 140

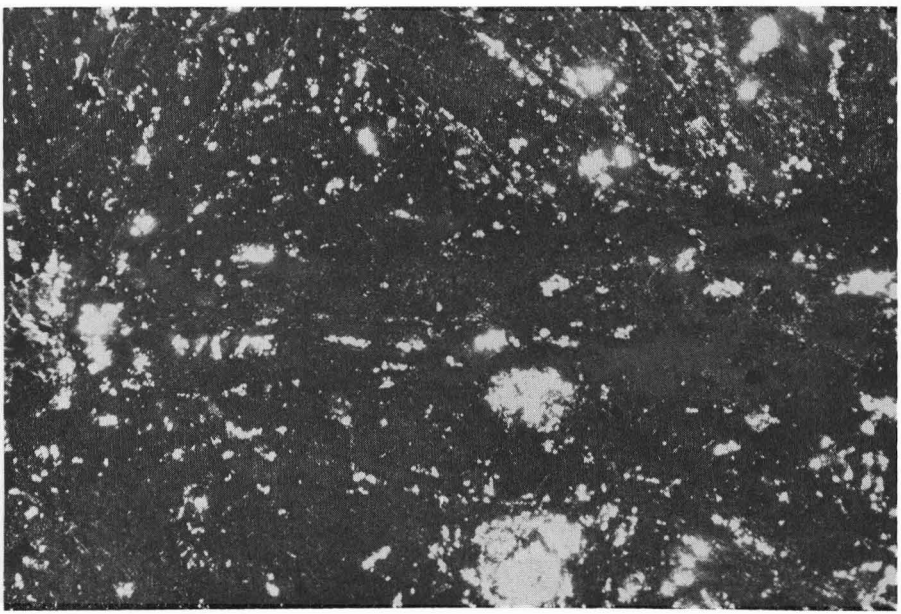

B. V-4 Lower Crossed-nicols × 140

PLATE 6. Completely halloysitized plagioclase with scattered aggregates of gibbsite.

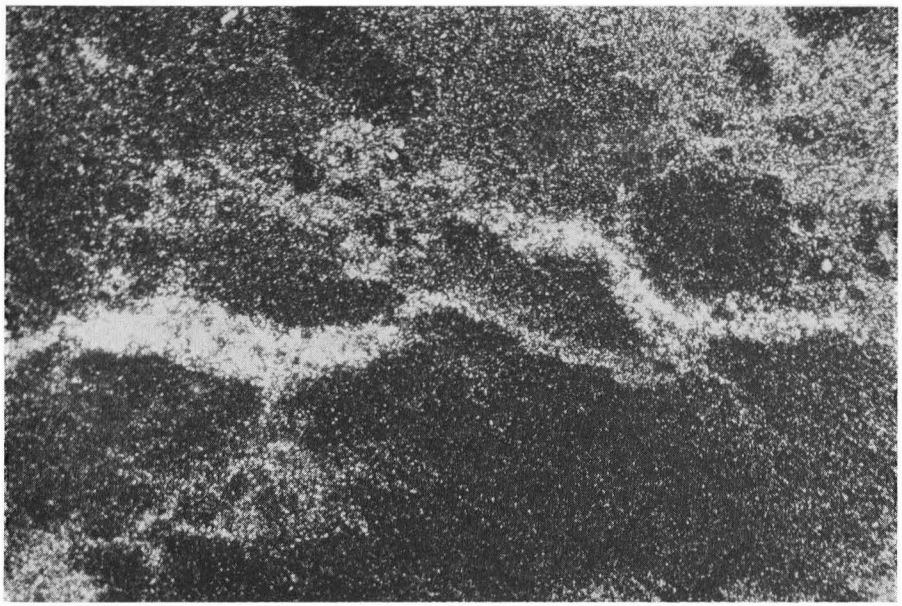

A. I-2 Crossed-nicols × 140

B. I-3 Crossed-nicols × 140

PLATE 7. A—Gibbsite aggregates appearing from an isotropic background.
B—Veinlet showing the typical translocated gibbsite formation.

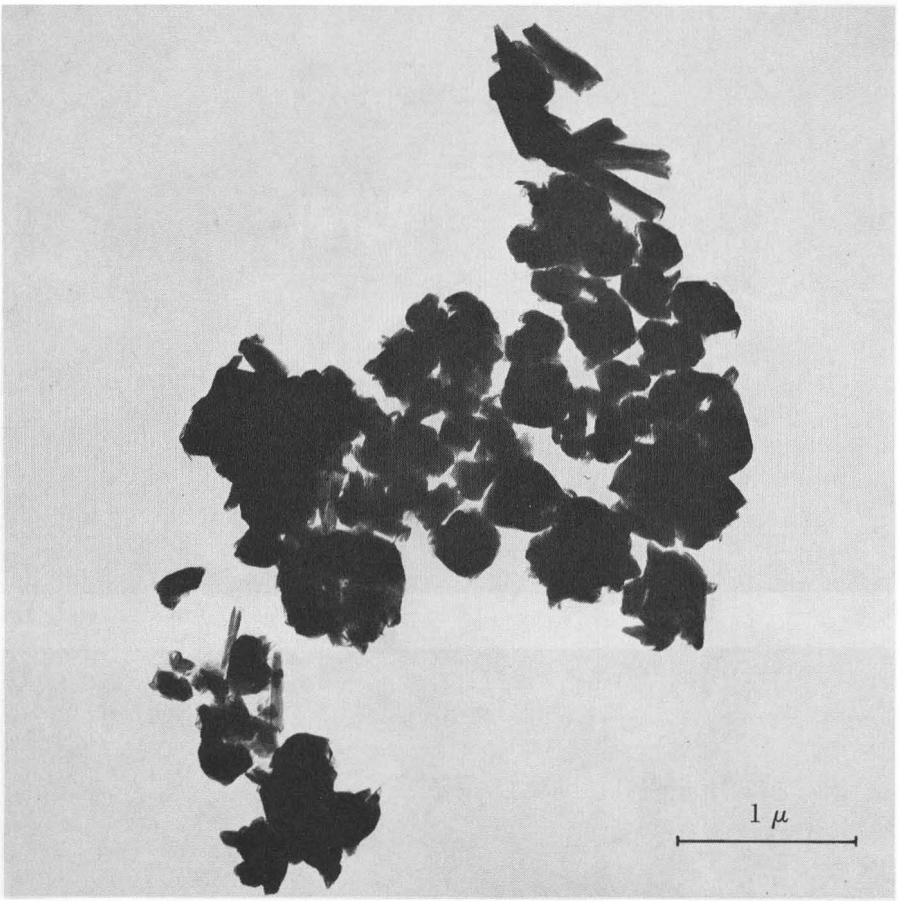

PLATE 8. Electron micrograph of Maui "standard" halloysite, a precipitation product.

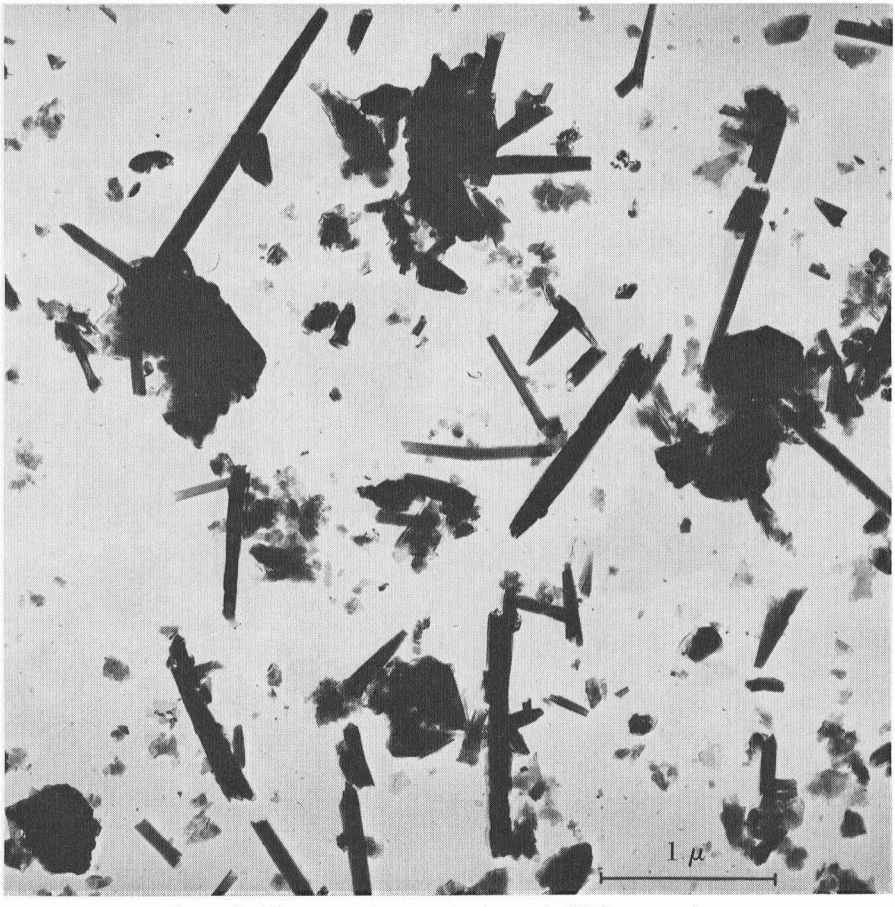

PLATE 9. Electron micrograph of sample VI-4, a saprolyte.

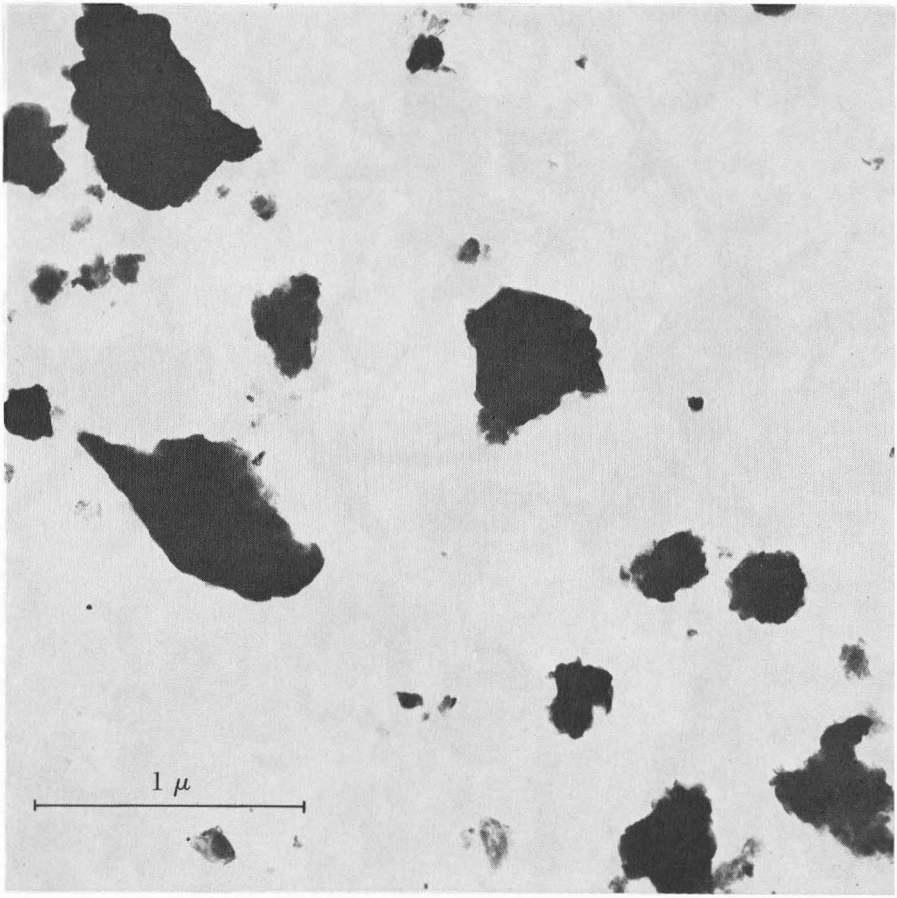

PLATE 10. Electron micrograph of sample V-3, a saprolyte.

indicate that halloysite formed as a residual weathering product is morphologically different from that formed as a precipitation product.

The micrograph of the standard halloysite for this study is shown in plate 8 and is similar to the halloysite described by Sudo and Takahashi (1955) and Birrell *et al.* (1955). The dominant particles of the clay give an appearance of not being completely spheroid in shape but having curled edges. Some of the rounded grains appear to be aggregates of tiny imperfectly tubular material. Some short tubular particles are also seen. Differential thermal and X-ray diffraction analyses previously made indicated, however, that all of the particles are halloysite. Pedro (1962), in his leaching experiments with basaltic rock fragments, found that the lessivate (leached phase), which contained 57.7% SiO_2, 23.2% Al_2O_3, 10.3% Na_2O, 9.6% K_2O, and 3.2% CaO+MgO, formed an "allophane"-type amorphous product. The halloysite is in much the same environment with a lessivate composed of silica and alumina relatively free from iron oxide, alkaline earths, and alkalies. The hydrated silica and alumina probably crystallized into halloysite through the intermediate step of allophane as Fieldes (1955) postulates.

The typical tubular halloysite particles described by Bates *et al.* (1950) are seen in the micrograph of sample VI-4, reproduced as plate 9. This sample was established through petrographic examination to be a residual mineral wherein the feldspars have weathered *in situ* to halloysite, probably with a gelatinous hydrous intermediary described by Murata (1946) and Fieldes and Swindale (1954).

The particles reproduced by the electron micrograph of sample V-3 on plate 10 showed no distinctive characteristics such as the tubular or rounded shapes of the halloysite samples previously discussed. Since other analyses of the sample showed it to be composed of gibbsite particles with very small amounts of halloysite and amorphous material, the micrograph of the sample may be interpreted to be gibbsite.

DISCUSSION

All of the experimental data reveal that mugearite weathers to halloysite where the texture of the rock permits unimpeded movement of silica-carrying solutions. Sample series V afforded an exception to the general pattern of weathering in that it had altered to both halloysite and gibbsite.

Since sample series V was located in an area adjoining a gibbsitic area, it is possible that leaching waters low in silica concentration caused its weathering to gibbsite rather than to halloysite as in the case of V-2 and V-3. However, if the fact that V-4 was composed almost entirely of halloysite is considered, this hypothesis becomes untenable. It is more likely that the dense rock impeded the movement of solutions thereby developing non-uniform micro-environments of high and low Si:Al ratio.

This may be explained in terms of the differential mobilities of silica and alumina and the concentration gradient of these ions within the rock. Pedro

(1962) has treated basaltic rock fragments with leaching waters of pure water and carbonic water and measured the residual as well as the leached phase for their products. He found that carbonic water favored the removal of silica over alumina (62.6% SiO_2 to 2.5% Al_2O_3), exceeding the ratio of silica to alumina in the original rock. Thus when a rock is subjected to intense leaching a rapid removal of silica takes place with the residual formation of gibbsite. Halloysite, on the other hand, might be expected to form in zones which can maintain a sufficient silica concentration gradient by having the outgoing silica equal the incoming silica. Such differences in the concentration gradient of silica can be set up in the rock in these narrow bands by the outward diffusion of ions and periodic concentration of them in small narrow bands thus giving rise to the observed complex weathering.

A careful study of any position in this profile will show gibbsite and halloysite along with noncrystalline material and resistant primary minerals. The variation in the mineral composition of this study area suggests that every stage of weathering can exist in micro-environments scattered throughout the weathering zone. All the weathering factors being equal, the ratio of the minerals in each micro-environment will depend on its position in the weathering profile, the difference in density and texture of the rock, and its proximity to a drainage channel and the content of the material in this drainage channel.

Thus when a rock is subjected to weathering which removes silica, residual gibbsite is formed. Halloysite will be maintained as the dominant mineral only as long as the supply of silica is maintained in the proper ratio to that of alumina by having the outgoing silica replaced by the incoming silica. The silica supply can be maintained as long as that weathering zone is proximate to an unweathered rock or a drainage channel of high silica material. This situation will not persist indefinitely. Eventually the silica from these adjacent sources will be depleted and the entire weathering zone will undergo desilication and result in bauxite formation.

In light microscopy studies of VI-3, -4, and -5, thin streaks of low white birefringence following the orientation of the groundmass feldspar and outlining the plagioclase phenocrysts and their cleavage faces were observed. These reticular lines do not have the characteristics of gibbsite. Other analyses also fail to indicate the presence of gibbsite in the samples. The birefringence may be caused by the presence of unweathered feldspars. It could also be caused by the presence of strained noncrystalline silica or alumina. Another possible explanation is that the reticular patterns may be due to pressure cutans formed by the partial orientation of nontubular halloysite. This feature might also be the result of oriented aggregates of kaolinite. However, no evidence for this mineral has been uncovered. The phenomenon must remain unexplained until further investigation using finer analytical techniques can be conducted.

Research presently being conducted in the Department of Agronomy and Soil Science on a soil profile from Aiea, Oahu, shows that the mineral in the

saprolyte zone is hydrated halloysite. The parent rock material is basalt. Differential thermal analyses by Walker *et al.* (1961) of the Kapaa soils on the bauxite reclamation area on the island of Kauai indicate that the saprolyte zone of these soils is composed of halloysite, gibbsite, and amorphous hydrous oxides. The reclamation site overlies the Koloa volcanic series which is composed of olivine basalt, nepheline basalt, and melilite-nepheline basalt. In East Maui, the saprolyte zone underlying the Haiku and Pauwela clay soils, which the authors are presently characterizing, is also composed of halloysite, gibbsite, and amorphous hydrated oxides of silicon, aluminum, iron, and titanium.

These examples show that irrespective of the parent rock material, the product of geologic weathering is halloysite and gibbsite. The gibbsite content increases with increasing rainfall. The iron-oxide content is dependent on the mafic mineral content of the parent rock. Thus the extensive and relatively pure halloysite formation on West Maui is due to the moderate rainfall of the area and to the high plagioclase and low mafic mineral content of the parent rock.

Sand (1956) postulated that muscovite or secondary mica is essential for the formation of residual kaolinite. If weathering is intense and good drainage leaches the potash, secondary mica formation is inhibited and the feldspathic rock is altered to hydrated halloysite. The observations on Hawaiian rock weathering corroborate Sand's hypothesis, for the plagioclase which comprises the feldspar content of Hawaiian rocks uniformly weathers to hydrated halloysite.

However, the same hypothesis cannot be extended into the pedologic weathering zone. Tamura (1951) recognized illite and hydrous clay intermediates in the A_1 and A_2 horizons of the Naiwa profile which is formed on the same mugearite flow a few miles away from the study area of this paper. The authors' present work in the mineral characterization of the soils of the Humic Ferruginous Latosol Group identifies kaolinite and illite in all but the most ferruginous soil of the Group.

Saing (1964) has studied a contiguous series of soils traversing the Koolau Range on the island of Oahu in the general vicinity of Wahiawa Plateau up to the summit of the Range. The soils encompassed a continuous sequence of the Hawaiian zonal soils which are the Low Humic Latosol, the Humic Ferruginous Latosol, the Humic Latosol, and a Hydrol Humic Latosol in order of ascending elevation. He presents an interesting inverse correlation between the kaolinite and illite content, with kaolinite being dominant in the drier soil and illite attaining dominance in the Humic Latosol and the Hydrol Humic Latosol soils.

Is there a relationship between these two minerals in the transformation from halloysite of the parent material to kaolinite of the soil solum? What are the variables introduced into the pedological weathering that forms kaolinite from a relatively uniform parent material composed of halloysite, gibbsite, and hydrated oxides which are devoid of the micaceous precursor

postulated as necessary for the formation of kaolinite? These are some of the questions that arise and call for further studies.

SUMMARY

The environment at Wailena Gulch at the northwest end of West Maui with an annual rainfall of 40 inches favors halloysite formation. The parent material is a very thick flow of mugearite composed of approximately 80% oligoclase feldspar, 12% ferromagnesium minerals, and 8% magnetite. This mineral assemblage accounts for the unique, relatively uncontaminated halloysite.

The vesicular rock weathers uniformly into pure halloysite. This uniform pattern is undoubtedly due to the unimpeded movement of solutions through the rock constantly maintaining a high silica environment. Within the dense rock, diverse micro-environments of small area are created. The plagioclase feldspars weather to gibbsite or halloysite depending on the concentration gradient of alumina and silica within these micro-environments.

Petrographic studies showed that in this study site gibbsite, once formed, is not resilicated to halloysite.

REFERENCES

1. Abbott, A. T.
   1958. occurrence of gibbsite on the island of kauai, hawaiian islands. Econ. Geol. 53: 842–853.

2. Bates, T. F.
   1962. halloysite and gibbsite formation in hawaii. In: clays and clay minerals. Natl. Acad. Sci.—Natl. Res. Council Publ. 9. Pp. 315–328.

3. Bates, T. F., F. A. Hildebrand, and A. Swineford.
   1950. morphology and structure of endellite and halloysite. Amer. Mineral. 35: 463–484.

4. Birrell, K. S., M. Fieldes, and K. I. Williamson.
   1955. unusual forms of halloysite. Amer. Mineral. 40: 122–124.

5. Dean, L. A.
   1947. differential thermal analysis of hawaiian soils. Soil Sci. 63: 95–105.

6. Fieldes, M.
   1955. clay mineralogy of new zealand soils, part ii: allophane and related mineral colloids. New Zealand J. Sci. Tech. Sec. B 37: 336–350.

7. Fieldes, M., and L. D. Swindale.
   1954. chemical weathering of silicates in soil formation. New Zealand J. Sci. Tech. Sec. B 36: 140–154.

8. Fujimoto, G., G. D. Sherman, and A. E. Chang.
   1948. the chemical composition of the separated mineral fractions of a ferruginous humic latosol profile. Soil Sci. Soc. Amer. Proc. 13: 166–169.

9. Hough, G. J., and H. G. Byers.
   1937. chemical and physical studies of certain hawaiian soil profiles. U. S. Dept. Agr. Tech. Bull. 584. 26 pp.

10. Hough, G. J., P. L. Gile, and Z. C. Foster.
    1941. rock weathering and soil profile development in the hawaiian islands. U. S. Dept. Agr. Tech. Bull. 752. 43 pp.

11. Macdonald, G. A.
    1949. hawaiian petrographic province. Bull. Geol. Soc. Amer. 60: 1541–1596.

12. McGeorge, W. T.
    1917. composition of hawaiian soil particles. Hawaii Agr. Exp. Sta. Bull. 42. 12 pp.

13. Murata, K. J.
    1946. significance of internal structure in gelatinizing silicate minerals. U. S. Geol. Surv. Bull. 1950. Pp. 25–33.

14. Pedro, G.
    1962. experimental research on the weathering of crystalline rocks and the geochemical characterization of pedogenetic phenomena. Trans. Joint Meeting Commissions IV & V, Internatl. Soc. Soil Sci. (Internatl. Soil Conf., New Zealand). Pp. 50–54.

15. Ross, C. S., and P. F. Kerr.
    1934. halloysite and allophane. U. S. Geol. Surv. Prof. Paper 185-G. Pp. 135–148.

16. Saing, Soe.
    1964. clarification of the nature of the kaolin minerals in hawaiian soils. M. S. Thesis, University of Hawaii. 70 pp.

17. Sand, L. B.
    1956. on the genesis of residual kaolins. Amer. Mineral. 41: 28–40.

18. SHERMAN, G. D., Z. C. FOSTER, and C. K. FUJIMOTO.
1948. SOME OF THE PROPERTIES OF THE FERRUGINOUS HUMIC LATOSOLS OF THE HAWAIIAN ISLANDS. Soil Sci. Soc. Amer. Proc. 13: 471–476.

19. SHERMAN, G. D., J. FUJIOKA, and G. FUJIMOTO.
1955. TITANIFEROUS FERRUGINOUS LATERITE OF MEYER LAKE, MOLOKAI, HAWAII. Pacif. Sci. 9: 49–55.

20. SHERMAN, G. D., and G. UEHARA.
1956. THE WEATHERING OF OLIVINE BASALT IN HAWAII AND ITS PEDOGENIC SIGNIFICANCE. Soil Sci. Soc. Amer. Proc. 20: 337–340.

21. STEARNS, H. T., and G. A. MACDONALD.
1942. GEOLOGY AND GROUND-WATER RESOURCES OF THE ISLAND OF MAUI, HAWAII. Hawaii Div. Hydrog. Bull 7. 344 pp.

22. SUDO, T., and H. TAKAHASHI.
1955. SHAPES OF HALLOYSITE PARTICLES IN JAPANESE CLAYS. In: CLAYS AND CLAY MINERALS. Natl. Acad. Sci.—Natl. Res. Council Publ. 456. Pp. 67–79.

23. TAMURA, T.
1951. MINERALOGICAL COMPOSITION OF A SOIL PROFILE FROM THE NAIWA FAMILY OF THE FERRUGINOUS HUMIC LATOSOL GROUP. M. S. Thesis, University of Wisconsin.

24. TAMURA, T., M. L. JACKSON, and G. D. SHERMAN.
1953. MINERAL CONTENT OF LOW HUMIC, HUMIC AND HYDROL HUMIC LATOSOLS OF HAWAII. Soil. Sci. Soc. Amer. Proc. 17: 343–346.

25. ———, ———, and ———.
1955. MINERAL CONTENT OF A LATOSOLIC BROWN FOREST SOIL AND A HUMIC FERRUGINOUS LATOSOL OF HAWAII. Soil Sci. Soc. Amer. Proc. 19: 435–439.

26. TANADA, T.
1951. CERTAIN PROPERTIES OF THE INORGANIC COLLOIDAL FRACTION OF HAWAIIAN SOILS. J. Soil Sci. 2: 83–96.

27. WALKER, J. L., W. E. HOLMES, and G. D. SHERMAN.
1961. THE BENEFICIATION OF GIBBSITIC SOILS OF THE KAPAA AREA. Hawaii Agr. Exp. Sta. Tech. Prog. Rept. 131. 12 pp.